Unified Multi-Modal Interactive & Reactive 3D Motion Generation via Rectified Flow

Anonymous authors

000

001

002003004

010 011

012

013

014

015

016

017

018

019

021

023

025

026

027 028 029

030

033

034

037

040 041

042 043

044

045

046

047

051

052

Paper under double-blind review

ABSTRACT

Generating realistic, context-aware two-person motion conditioned on diverse modalities remains a central challenge in computer graphics, animation, and human-computer interaction. We introduce DualFlow, a unified and efficient framework for multi-modal two-person motion generation. DualFlow conditions 3D motion synthesis on diverse inputs, including text, music, and prior motion sequences. Leveraging rectified flow, it achieves deterministic straight-line sampling paths between noise and data, reducing inference time and mitigating error accumulation common in diffusion-based models. To enhance semantic grounding, DualFlow employs a Retrieval-Augmented Generation (RAG) module that retrieves motion exemplars using music features and LLM-based text decompositions of spatial relations, body movements, and rhythmic patterns. We use contrastive objective that further strengthens alignment with conditioning signals and introduce synchronization loss that improves inter-person coordination. Extensive evaluations across text-to-motion, music-to-motion, and multi-modal interactive benchmarks show consistent gains in motion quality, responsiveness, and efficiency. DualFlow produces temporally coherent and rhythmically synchronized motions, setting state-of-the-art in multi-modal human motion generation. We will release the code upon acceptance.

1 Introduction

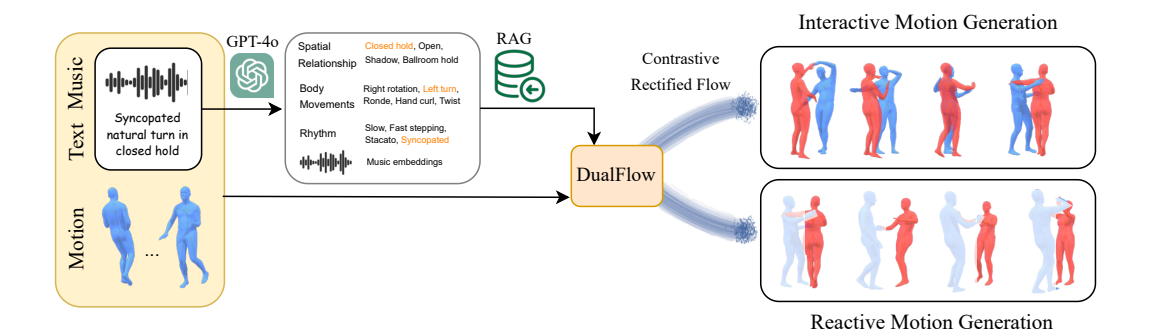


Figure 1: Our DualFlow model unifies two tasks: (a) Interactive Motion Generation, which synthesizes synchronized two-person interactions, (b) Reactive Motion Generation, which generates responsive motions for Person B (red) conditioned on Person A's (blue) movements. The generation process is conditioned jointly on text, music, and the retrieved motion samples.

Generating realistic, context-aware interactive human motion remains a core challenge in computer graphics, animation, and human-computer interaction (Holden et al., 2016; Duan et al., 2022). Synthesizing coordinated motion between two individuals introduces unique complexities requiring models to capture mutual responsiveness, physical plausibility, and rich interpersonal dynamics (Cao et al., 2023). Since human interactions are often driven by multi-modal stimuli such as language, music, and physical cues, generative systems must interpret and integrate diverse inputs to enable immersive virtual experiences, intelligent avatars, and responsive human-robot collaboration

(Tevet et al., 2022). Recent advances in deep generative models, particularly diffusion-based approaches, have shown strong performance in motion generation (Zhang et al., 2023b), but remain limited by high computational cost, error accumulation over long sequences, and weak real-time reactivity (Guo et al., 2022; Lu et al., 2022). These constraints hinder their applicability in interactive systems such as virtual avatars, social robotics, and dance simulation, where low-latency and seamless coordination are essential.

To overcome these challenges, we propose DualFlow, a multi-modal rectified flow framework that unifies interactive and reactive motion generation within a single architecture. Instead of designing separate models for each task, DualFlow employs cascaded DualFlow Blocks that flexibly adapt through a masking mechanism: both branches remain active for interactive generation, while the reactor branch alone is conditioned on the actor's motion for reactive synthesis. This design enables seamless switching between tasks without retraining while preserving temporal coherence and interpersonal synchronization. By integrating retrieval-augmented conditioning from music and text with structured cross-attention modules, DualFlow captures fine-grained spatial relationships, rhythmic cues, and semantic intent. In doing so, it directly addresses the shortcomings of existing diffusion-based approaches, offering a scalable, context-aware framework capable of real-time responsiveness in multi-person, multi-modal scenarios.

Our key contributions are: (1) The first unified architecture for interactive two-person and reactive motion generation. (2) A Retrieval-Augmented Generation (RAG) framework leveraging music features and LLM-based text decompositions (spatial relationship, body movement, rhythm) to guide semantically faithful motion synthesis. (3) Contrastive Rectified Flow generation, improving motion quality, diversity, and alignment with conditioning signals. (4) Extensive quantitative, qualitative, and ablation studies on diverse two-person datasets, showing DualFlow generates coherent, expressive, and contextually appropriate motions with fewer steps. Importantly, our approach outperforms state-of-the-art baselines by 2.5% in FID, 76% in R-precision, and 3x in Multi-Modal Distance for Interactive task and 1.7% in FID, 2.5x in R-precison and 2x in Multi-Modal Distance for Reactive task on MDD Dataset, establishing a new benchmark for multi-person, multi-modal motion generation.

2 Related Work

Two-person Motion Generation. While single-person motion generation has advanced rapidly (Guo et al., 2022; Tevet et al., 2022; Petrovich et al., 2022; Zhang et al., 2024), extending these methods to multi-person settings introduces the additional challenge of modeling coordination between agents. Early two-person models (Kundu et al., 2020; Xu et al., 2023; Xie et al., 2021) demonstrated feasibility but exhibited limited generalization. To address data scarcity and modeling complexity, Liang et al. (2024) introduced a large-scale interaction dataset with a text-conditioned diffusion model, later extended by text-guided variants (Shafir et al., 2024; Yi et al., 2024; Li et al., 2024a). In the domain of dance, specialized frameworks explored music-conditioned lead-follower generation (Li et al., 2024b; Wang et al., 2025; Ghosh et al., 2025). Despite these advances, most diffusion-based methods remain slow and restricted to single-modality conditioning. For reactive motion generation, early GAN- and transformer-based methods (Men et al., 2022; Rahman et al., 2022; Ghosh et al., 2024) have recently been extended with text (Xu et al., 2024; Cen et al., 2025) or with joint leader motion and music for dance accompaniment (Siyao et al., 2024). However, these approaches still suffer from high inference latency and limited multi-modal support. Our framework, DualFlow, addresses these challenges by unifying interactive and reactive motion generation within a single transformer-based architecture, jointly conditioned on text and music.

Retrieval-Augmented Generation (RAG). Adding RAG has improved generation quality across LLMs (Gao et al., 2023; Guu et al., 2020; Lewis et al., 2020), image (Blattmann et al., 2022; Chen et al., 2022; Sheynin et al., 2022), and video tasks (He et al., 2023). RAG has been applied to text-to-motion generation (Zhang et al., 2023a; Kalakonda et al., 2025; Liao et al., 2024; Petrovich et al., 2023; Bensabath et al., 2024); however, these efforts focus on single-person motion. DualFlow is the first framework to extend RAG to interaction-aware retrieval for multi-person motion generation.

Diffusion and Rectified Flow Models. Diffusion models like MDM (Tevet et al., 2022), MotionDiffuse (Zhang et al., 2024), and MoFusion (Dabral et al., 2023) have succeeded in motion generation but require hundreds of denoising steps, making real-time use impractical. Alternatives such as

MotionMatch (Hu et al., 2023) and FlowMotion (Canales Cuba & Gois, 2025) use Flow Matching (Lipman et al., 2023) to avoid iterative sampling but face scaling and optimization challenges. We introduce DualFlow, built on Rectified Flow (Liu et al., 2022), which simplifies training by using straight-line transport between noisy and clean data, yielding faster and more stable sampling.

3 METHODS

3.1 PROBLEM FORMULATION

A two-person motion interaction $\mathbf{x} \in \mathcal{X}_{\mathcal{A}} \times \mathcal{X}_{\mathcal{B}}$ is represented as person A's motion $\mathbf{x_a} = \{x_a^i\}_{i=1}^N$ and person B's motion $\mathbf{x_b} = \{x_b^i\}_{i=1}^N$, where paired frames $x^j = (x_a^j, x_b^j)$ are naturally synchronized. For the asymmetric case, person A is the *Actor* and person B the *Reactor*. The motion space is $\mathcal{X} \subset \mathbb{R}^{N \times J \times 3}$, with N frames and J joints. Music features lie in $\mathcal{M} \subset \mathbb{R}^{N \times d_m}$ with dimension d_m , and text embeddings in $\mathcal{C} \subset \mathbb{R}^{d_c}$ with dimension d_c .

Interactive Motion Generation. Given text $c \in \mathcal{C}$ and/or music $m \in \mathcal{M}$, the task is to generate synchronized two-person motion $(\mathbf{x_a}, \mathbf{x_b})$ aligned with both modalities: $F(c, m) \mapsto \mathbf{x}$ Special cases include text-only $(m = \phi)$ (Liang et al., 2024), music-only $(c = \phi)$ (Li et al., 2024b; Ghosh et al., 2025)), and joint text-music conditioning defined as Text-to-Duet by Gupta et al. (2025).

Reactive Motion Generation. Given the actor's motion $\mathbf{x_a} \in \mathcal{X}$, text $c \in \mathcal{C}$, and/or music $m \in \mathcal{M}$, the goal is to generate the reactor's motion $\mathbf{x_b} \in \mathcal{X}$ such that $(\mathbf{x_a}, \mathbf{x_b})$ are coherent and synchronized: $G(c, m, \mathbf{x_a}) \mapsto \mathbf{x_b}$. Variants include text-only $(m = \phi)$ (Xu et al., 2024), music-only $(c = \phi)$ (Siyao et al., 2024), and joint text-music conditioning defined as Text-to-Dance Accompaniment by Gupta et al. (2025).

Human Motion Representation. We represent motion in a global coordinate system, where the origin is anchored at the root joint of person A. The position of person B is expressed relative to this root, ensuring a unified spatial reference frame for both. Our motion representation is based on the format introduced by Liang et al. (2024), and encodes a single frame of an individual's motion as $x^i = [j_g^p, j_g^v, j^r, c^f]$. Each frame includes global joint positions $j_g^p \in \mathbb{R}^{3N_j}$, global joint velocities $j_g^v \in \mathbb{R}^{3N_j}$, local joint rotations $j^r \in \mathbb{R}^{6(N_j-1)}$ in 6D format within a root-relative coordinate frame, and binary foot contact indicators $c^f \in \mathbb{R}^4$ that specify ground contact status for each foot joint at that time step. To model body joint rotations, we use the SMPL model (Loper et al., 2015) with $N_j = 22$ joints, resulting in a fixed input dimension of $x_i \in \mathbb{R}^{262}$.

3.2 MULTI-MODAL MOTION RETRIEVAL

Retrieval Dataset. Direct retrieval from raw text often overlooks the nuanced dimensions of interactive human motion, yielding low diversity or biased matches. To address this, we use GPT-4o (Hurst et al., 2024) to decompose each prompt into three focused descriptions, inspired by Laban Movement Analysis (Laban, 1950) and aligned with the MDD Dataset (Gupta et al., 2025): (1) **Spatial Relationship** (proximity, orientation, handholds), (2) **Body Movement** (actions, body parts, posture), and (3) **Rhythm** (timing, musicality, stepping). To achieve high-quality and consistent decomposition, we design a structured prompting framework for the LLM (details in Appendix). For each category, we build retrieval databases using CLIP (Radford et al., 2021) embeddings (D^S, D^B, D^R) and music embeddings (D^M) from Jukebox (Dhariwal et al., 2020).

Similarity Scoring. We generalize the similarity scoring function introduced by Zhang et al. (2023a) for any modality q. For a given query sample p with modality-specific feature embedding f_p^q , and a candidate database motion sample \mathbf{x}_i with embedding f_i^q and motion length l_i , the similarity score s_i^q is computed as:

$$s_i^q = \langle f_i^q, f_p^q \rangle \cdot e^{-\lambda \cdot \frac{|l_i - l_p|}{\max\{l_i, l_p\}}} \tag{1}$$

where $\langle\cdot,\cdot\rangle$ is cosine similarity and the exponential term penalizes mismatch across motion length with sensitivity λ , allowing retrievals that are semantically aligned and temporally compatible. Using this scoring, we retrieve top-k matches from each database for every sample, yielding sets $(R_i^S, R_i^B, R_i^R, R_i^M)$ as shown in Fig. 2. The retrieved sets collectively offer a diverse yet semantically relevant collection of motion exemplars, which are later used to guide generation.

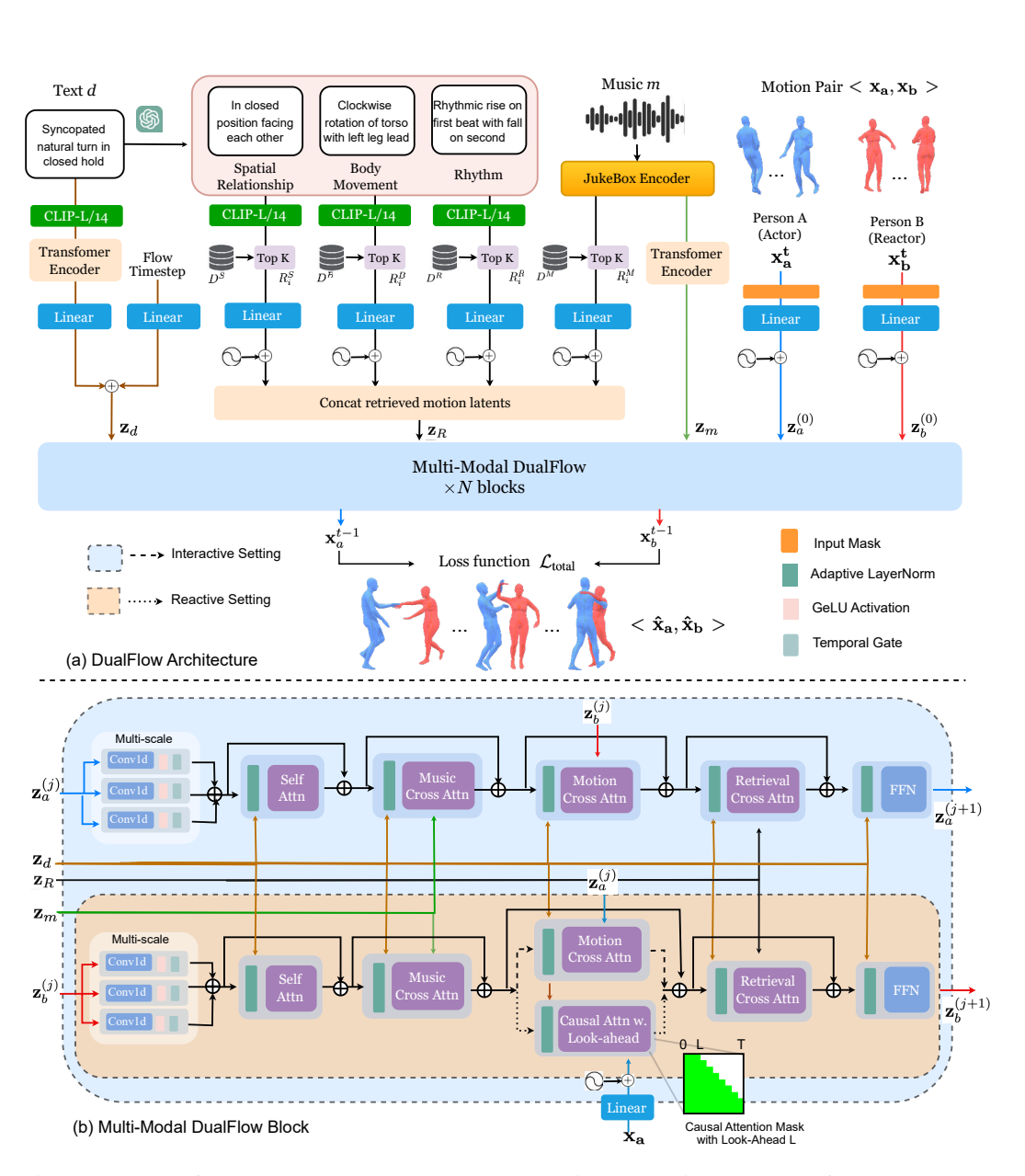


Figure 2: (a) Our framework takes text (CLIP-L/14), music, and motion sequences from an actor (A) and reactor (B) as inputs. Motion samples are retrieved using music features and LLM-decomposed text cues (spatial relationship, body movement, rhythm). These modality-specific latents are processed by cascaded Multi-Modal DualFlow Blocks that model interactive dynamics. Outputs are either both actors' motions (interactive) or only the reactor's motion (reactive) via a masking mechanism. (b) A DualFlow Block: in the interactive setting, both branches operate symmetrically with Motion Cross Attention coordinating joint motion; in the reactive setting, the actor branch is masked and the reactor branch employs a Causal Cross Attention module with Look-Ahead L, replacing Motion Cross Attention, to condition on the actor's motion.

3.3 Model Architecture

Conditioning latents. The text description d is encoded using a pretrained CLIP model (Radford et al., 2021) followed by a transformer encoder, then linearly projected and fused with time-step embeddings to form the text latent \mathbf{z}_d . Similarly, the music input m is processed by a pretrained Jukebox encoder (Dhariwal et al., 2020), linearly transformed, and passed through a transformer encoder to obtain the music latent \mathbf{z}_m . For retrieval-based conditioning, we use four retrieved motion sets $(R_i^S, R_i^B, R_i^R, R_i^M)$ corresponding to spatial, body, rhythm, and music cues. Positional encodings and a shared linear projection map these samples to the motion latent space, and the resulting features are concatenated into the aggregated retrieval latent \mathbf{z}_R .

Model Pipeline. Motion inputs \mathbf{x}_a^t and \mathbf{x}_b^t sampled for time step t are first projected through individual linear layers, followed by the addition of positional encodings, resulting in initial motion latents $\{\mathbf{z}_a^{(0)}, \mathbf{z}_b^{(0)}\}$. They are fed into the main pipeline consisting of N cascaded DualFlow blocks. The first block takes the initial motion latents $\{\mathbf{z}_a^{(0)}, \mathbf{z}_b^{(0)}\}$ as input. Each subsequent block (j+1) takes the outputs from the previous block $\{\mathbf{z}_a^{(j)}, \mathbf{z}_b^{(j)}\}$ and produces updated latents $\{\mathbf{z}_a^{(j+1)}, \mathbf{z}_b^{(j+1)}\}$, where $j \in \{0, 1, \dots, N-1\}$. All blocks are jointly conditioned on the multi-modal context $\{\mathbf{z}_d, \mathbf{z}_m, \mathbf{z}_R\}$. The output from the last block, $\{\mathbf{x}_a^{t-1}, \mathbf{x}_b^{t-1}\}$, gives the denoised motion.

DualFlow Block. Each DualFlow block refines motion representations through temporally-aware and context-conditioned operations. It begins with a multi-scale temporal convolution module with varying kernel sizes to capture motion patterns at different time resolutions, followed by a GELU activation (Hendrycks & Gimpel, 2023). Branch outputs are adaptively fused using learnable gating weights γ_k . The representation then passes through a Self-Attention layer to model internal temporal dependencies, followed by a structured sequence of Cross-Attention layers: (1) *Music Cross-Attention* to align motion with music latent \mathbf{z}_m , (2) *Motion Cross-Attention* to capture interperson interaction which gets replaced by *Casual Cross-Attention with Look-Ahead* during reactive setting and (3) *Retrieval Cross-Attention* to semantically guide generation using retrieved exemplars. All modules use residual connections for stability, and the text latent \mathbf{z}_d is injected via LayerNorm conditioning. Each block thus integrates temporal structure, musical rhythm, and semantic guidance from retrieval. Please refer to Appendix for detailed description of each module.

Task settings. In the interactive setting, both \mathbf{x}_a^t and \mathbf{x}_b^t are sampled for time step t as input. In the reactive setting, only the reactor's motion \mathbf{x}_b is sampled, while the actor's motion \mathbf{x}_l is masked on the input side and used for conditioning. To enable anticipatory reactor response, the *Motion Cross-attention* is switched with Causal Cross Attention Layer having a Look-Ahead parameter L. It uses an upper triangular mask such that reactor's motion attends to past and only L future frames of the actor's motion (Fig.2). This look-ahead mechanism esnures temporally aligned and context-aware reactive generation.

3.4 Contrastive Rectified Flow

To generate realistic and semantically grounded duet motions, we build upon the Rectified Flow Matching framework (Liu et al., 2022) and augment it with a contrastive learning objective inspired by Contrastive Flow Matching Stoica et al. (2025). Unlike traditional diffusion models that rely on stochastic denoising, rectified flow formulates the generation process as a deterministic Ordinary Differential Equation (ODE) that transports a noise sample toward a data sample along a straightline path in motion space. Given a ground truth motion sample \mathbf{x}_0 and a noise sample $\epsilon \sim \mathcal{N}(0, \mathbf{I})$, the interpolated state at time $t \in [0,1]$ is defined as: $\mathbf{x}_t = (1-t)\mathbf{x}_0 + t\epsilon$, and $\mathbf{v}_t = \epsilon - \mathbf{x}_0$, where \mathbf{x}_t lies along the linear path between \mathbf{x}_0 and $\boldsymbol{\epsilon}$, and \mathbf{v}_t is the constant velocity vector guiding the transport. We train a time-dependent neural velocity field $\mathbf{v}_{\theta}(\mathbf{x}_{t},t,c)$ to approximate \mathbf{v}_{t} , conditioned on a multimodal context $c = (d, m, R_i^S, R_i^B, R_i^R, R_i^M)$, which includes the text description d, music segment m, and retrieved motion sets. This context is encoded using cross attention layers in DualFlow Block. The flow loss $\mathcal{L}_{\text{flow}}$ is obtained by minimizing the squared error between the predicted and target velocity: $\mathcal{L}_{\text{flow}} = \mathbb{E}_{\mathbf{x}_0, \boldsymbol{\epsilon}, t} \left| \left\| \mathbf{v}_{\theta}(\mathbf{x}_t, t, c) - \mathbf{v}_t \right\|_2^2 \right|$, To encourage semantic alignment, we introduce a triplet contrastive loss that enforces proximity in velocity space for semantically similar prompts: $\mathcal{L}_{\text{triplet}} = \mathbb{E}\left[\max\left(0, d(\hat{\mathbf{v}}, \mathbf{v}^+) - d(\hat{\mathbf{v}}, \mathbf{v}^-) + m\right)\right]$, where $d(\cdot, \cdot)$ denotes cosine distance, $\hat{\mathbf{v}}$ is the predicted velocity, \mathbf{v}^+ and \mathbf{v}^- are positive and negative velocity samples drawn from similar and dissimilar genres or text prompts, and m is the margin. This loss pushes the model to produce velocity fields that reflect the temporal structure of motion and the underlying semantics of the input, thereby improving generalization and sample diversity. We define contrastive flow loss \mathcal{L}_{CRF} that combines both losses: $\mathcal{L}_{CRF} = \mathcal{L}_{flow} + \lambda_{triplet} \mathcal{L}_{triplet}$, where $\lambda_{triplet}$ is weighting hyperparameter balancing reconstruction and semantic alignment objective.

3.5 REGULARIZATION LOSSES

Geometric Losses. We adopt the common geometric losses for human motion such as foot contact loss $\mathcal{L}_{\text{foot}}$ and joint velocity loss \mathcal{L}_{vel} from MDM Tevet et al. (2022) and bone length loss \mathcal{L}_{BL} from InterGen Liang et al. (2024). The geometric loss is defined as:

$$\mathcal{L}_{geo} = \mathcal{L}_{foot} + \lambda_{vel} \mathcal{L}_{vel} + \lambda_{BL} \mathcal{L}_{BL}$$
 (2)

where the hyper-parameters λ_{vel} , λ_{BL} are appropriately calibrated to fix the importance of each term.

Interaction Losses. We adapt joint distance map loss \mathcal{L}_{DM} and relative orientation loss \mathcal{L}_{RO} from InterGen Liang et al. (2024) that allows close interactions when dancers should be in contact as well as maintain proper facing directions and body alignments. To further enhance inter-person coordination in duet generation, we introduce synchronization loss \mathcal{L}_{sync} that explicitly allows spatial coherence between the actor and reactor by weighting pairwise joint distances based on both anatomical proximity and task-relevant importance:

$$\mathcal{L}_{\text{sync}} = \sum_{j_1, j_2} w_{\text{d}}(j_1, j_2) \cdot w_{\text{j}}(j_1, j_2) \cdot \|d_{\text{p}}(j_1, j_2) - d_{\text{gt}}(j_1, j_2)\|^2$$
(3)

Here, $d_{\rm p}(j_1,j_2)$ and $d_{\rm gt}(j_1,j_2)$ denote the predicted and ground truth Euclidean distances between joints of both dancers. The distance weight parameter $w_{\rm d}(j_1,j_2)$ assigns higher importance to spatially closer joint pairs (e.g., hands, shoulders), while joint weighting parameter $w_{\rm joint}(j_1,j_2)$ emphasizes end-effectors (e.g., feet, hips). The interaction loss $\mathcal{L}_{\rm sync}$ is obtained as:

$$\mathcal{L}_{inter} = \mathcal{L}_{DM} + \lambda_{RO} \mathcal{L}_{RO} + \lambda_{sync} \mathcal{L}_{sync}$$
(4)

where the hyper-parameters λ_{RO} and λ_{sync} are fixed based on importance of each term. For reactive setting, ground-truth actor's motion is used for all Interaction Losses.

Total Loss. The complete training objective combines all components through balanced weighting:

$$\mathcal{L}_{\text{total}} = \mathcal{L}_{\text{CRF}} + \lambda_{\text{geo}} \mathcal{L}_{\text{geo}} + \lambda_{\text{inter}} \mathcal{L}_{\text{inter}}$$
 (5)

where the hyperparameters λ_{geo} and λ_{inter} are meticulously selected to regulate the magnitude of their corresponding terms.

4 RESULTS

Datasets. We train and evaluate DualFlow on three widely used two-person motion datasets spanning text-to-motion, music-to-dance, and multi-modal duet generation: (1) **InterHuman-AS** (Xu et al., 2024), an asymmetric extension of InterHuman (Liang et al., 2024) with actorreactor labels, over 50K interaction clips across 11 action types (e.g., handshake, hug) and paired SMPL-X Pavlakos et al. (2019) sequences for modeling fine-grained interpersonal dynamics. (2) **DD100** (Siyao et al., 2024), featuring 100 duet dance routines (e.g., salsa, hip-hop, waltz) with high-resolution motion capture, paired music, and manually annotated dance structure for rhythm and style alignment. (3) **MDD** (Gupta et al., 2025), a large-scale multi-modal duet dance dataset with 10.3 hours of marker-based capture and 10K+ text annotations covering spatial relationships, choreography, movement quality, and music synchronization. Together, these datasets enable robust learning and evaluation of both interactive-reactive motion generation across multiple modalities.

Implementation Details. DualFlow consists of 20 cascaded blocks with 8 attention heads and dropout of 0.1. Both motion and conditioning inputs are projected into a 512-dimensional latent space, and each block's feedforward layer is set to size 1024. We use 4800-d Jukebox (Dhariwal et al., 2020) features for music and 768-d CLIP (ViT-L/14) (Radford et al., 2021) text embeddings. All cross-attention layers adopt Flash attention for faster processing. The stride values for the parallel convolution layers used are 7, 11 and 21. The model is trained with Contrastive Rectified Flow

using 200 integration steps and a cosine β scheduler. Training uses Adam with $\ln 2 \times 10^{-4}$, weight decay 2×10^{-5} , 1000 warm-up steps, batch size 32, for 5000 epochs. In the reactive setting, we use a 10-frame look-ahead. For classifier-free guidance, both modalities are masked 10% of the time, and text/music individually 20%. All hyperparameters were selected empirically on a held-out validation set.

Evaluation Metrics. We evaluate models using metrics adapted from text-to-motion (Liang et al., 2024) and music-to-motion (Siyao et al., 2024): *Frechet Inception Distance (FID)*: Distributional similarity between ground truth and generated motions; *Multimodal Distance (MM Dist)*: Text-motion alignment via feature distance; *R-Precision*: Text-motion alignment through retrieval accuracies within a batch; *Diversity*: Variety of generated motions regardless of conditions; *Multimodality (MModality)*: Diversity of generated motions under identical conditioning; *Beat Echo Degree (BED)*: Synchronization index of the both person's generated motion; and *Beat-Alignment Score (BAS)*: Alignment between inflection points in motion and musical beats.

4.1 QUANTITATIVE METRICS

Text & Music condition Motion Generation on MDD. We evaluate DualFlow on MDD, InterHuman-AS, and DD100 using standard text-motion and music-motion metrics. As shown in Table 1, DualFlow consistently outperforms baselines across most metrics for duet and reactive tasks. In the interactive task, DualFlow (Both) achieves the highest R-Precision@3 (0.513) and lowest MMDist (0.513), indicating strong alignment with multimodal inputs. DualFlow (Text) records the best Beat-Align Score (BAS) at 0.215. While InterGen (Text) attains the best FID (0.405) and Diversity (1.405), DualFlow (Both) follows closely with an FID of 0.415 and a Diversity score of 1.307. For the reactive task, DualFlow (Both) leads in all R-Precision scores, FID (0.686), MMDist (1.056), and shows strong BAS (0.228). Although DuoLando (Both) has a slightly higher BED (0.395), DualFlow remains competitive at 0.215.

Table 1: Duet Generation results on MDD dataset with both text and music modalities. **Bold** for best, underline for second best.

Methods	R	Precisio	n↑	FID↓	$\mathbf{MMDist} \!\!\downarrow$	$\mathbf{Diversity}{\rightarrow}$	$MModal \uparrow$	BED ↑	BAS↑
	Top 1	Top 2	Top 3						
Ground Truth	0.231	0.398	0.522	0.065	0.077	1.387	-	0.327	0.170
Duet Task									
MDM(Text) MDM(Music) MDM(Both)	0.082 0.041 0.061	0.124 0.102 0.108	0.192 0.135 0.163	1.420 2.241 1.739	2.133 2.471 2.244	1.216 1.192 1.235	0.811 0.411 0.787	0.211 0.210 0.194	0.186 0.192 0.190
InterGen(Text) InterGen(Music) InterGen(Both)	0.113 0.023 0.105	0.223 0.067 0.206	0.305 0.088 0.302	0.405 2.014 0.426	1.462 2.526 1.532	1.405 1.300 1.380	1.231 1.768 1.352	0.422 0.364 <u>0.385</u>	0.194 0.163 0.185
DualFlow(Text) DualFlow(Music) DualFlow(Both)	0.211 0.172 <u>0.185</u>	0.365 0.308 0.373	0.492 0.452 0.513	0.657 0.694 <u>0.415</u>	0.521 1.244 0.513	1.239 1.319 1.392	1.569 1.109 1.467	0.288 0.308 0.286	0.215 0.180 0.179
Reactive Task									
DuoLando(Text) DuoLando(Music) DuoLando(Both)	0.047 0.069 0.078	0.121 0.141 0.156	0.182 0.202 0.219	1.538 0.721 <u>0.698</u>	2.811 2.633 2.113	1.422 1.390 1.371	- - -	0.311 0.305 0.395	0.195 0.216 0.224
DualFlow(Text) DualFlow(Music) DualFlow(Both)	0.143 0.135 0.189	0.284 0.260 0.341	0.450 0.397 0.471	0.741 0.750 0.686	1.365 1.672 1.056	1.379 1.460 1.203	1.667 1.976 1.473	0.229 0.195 0.215	0.228 0.202 <u>0.226</u>

Text-conditioned Motion Generation on InterHuman-AS. Table 2 shows DualFlow significantly outperforms InterGen on R-Precision (Top-1: 0.437, Top-3: 0.681), with much lower MMDist (0.394) and the highest multimodality score (2.729). While InterGen has a slightly better FID (5.918 vs. 6.296), DualFlow offers better semantic and multimodal alignment. In the reactive task, DualFlow surpasses ReGenNet in R-Precision@3 (0.629 vs. 0.407), MMDist (6.230 vs. 6.860), and Multimodality (2.616 vs. 2.391), with a competitive FID (2.448).

Table 2: Interactive Two-person Generation results conditioned on text modality for the InterHuman-AS dataset.

Methods	R-Precision ↑		FID↓	MMDist↓	$\mathbf{Diverse} {\rightarrow}$	MModal↑	
	Top 1	Top 2	Top 3				
Ground Truth	0.452	0.610	0.701	0.273	3.755	7.948	-
Duet Task							
InterGen	0.371	0.515	0.624	5.918	5.108	7.387	2.141
DualFlow	0.437	0.558	0.681	6.296	4.394	<u>7.116</u>	2.729
Reactive Task							
ReGenNet	-	-	0.407	2.265	6.860	5.214	2.391
DualFlow	0.419	0.549	0.629	2.448	6.230	4.981	2.616

Figure 3: User study results

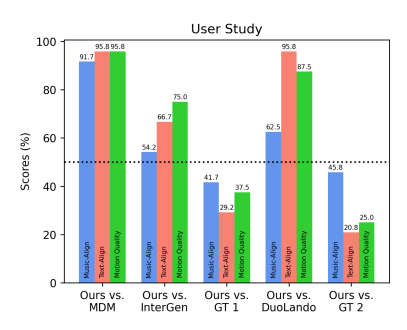
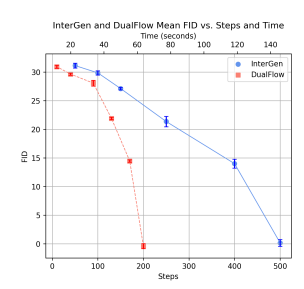


Table 3: Reactive Motion Generation results conditioned on text modality for the DD100 dataset.

	Solo Metrics				Inter	Rhythmic		
Methods	$\mathbf{FID}_k \downarrow$	$\mathbf{FID}_g{\downarrow}$	$\mathbf{Div}_k \!\!\uparrow$	$\mathbf{Div}_g \! \uparrow$	$ extbf{FID}_{cd}\!\!\downarrow$	$\mathbf{Div}_{cd}{\uparrow}$	$\overline{BED(\uparrow)}$	$\text{BAS}(\uparrow)$
Ground Truth	6.56	6.37	11.31	7.61	3.41	12.35	0.5308	0.1839
Bailando	78.52	36.19	11.15	7.92	6643.31	52.50	0.1831	0.1930
EDGE	69.14	44.58	8.62	6.35	5894.45	60.62	0.1822	0.1875
Duolando	25.30	33.52	10.92	7.97	9.97	14.02	0.2858	0.2046
DualFlow	19.22	28.85	11.01	7.35	5.57	19.52	0.2767	0.2113

Figure 4: FID vs. Steps



Reactive Motion Generation on DD100. Table 3 highlights DualFlow's performance across all metrics for reactive motion task. It achieves the best FID_k (19.22), FID_g (28.85), and FID_{cd} (5.57), with strong diversity and rhythmic scores (Div_k: 11.01, BAS: 0.211). While Duolando leads in BED (0.285), DualFlow follows closely at 0.276, showing generative fidelity and collaborative modeling.

4.2 QUALITATIVE EVALUATION

Fig. 5 shows a Qualitative Comparison for two samples from MDD Dataset. While samples generated from both text and music condition-based InterGen and DualFlow models follow the text prompt, the motion quality of InterGen has reduced motion quality as circled, where the hands are flipping and the distance is increased. We also conduct a user study to qualitatively evaluate the motion sequences generated by our DualFlow framework in comparison with baseline methods on both tasks from the MDD dataset (details in Appendix). As shown in Fig.3, DualFlow outperforms the baseline methods across most comparisons, demonstrating superior alignment with both text and music, as well as high-quality motion generation. Figure 4 illustrate how DualFlow model generates a 10 second long, 30 FPS, two person motion sequence with low FID within 200 steps. Meanwhile InterGen with diffusion requires upto 500 steps to achieve similar performance. This efficient inference allows rectified flow based models with faster sampling and reduced latency..

4.3 ABLATION STUDY

We perform an ablation study on both the tasks (Table 4) to assess the impact of key DualFlow components. We compare the full model against four variants: (1) replacing Causal Look-Ahead (CLA) Attention with regular cross-attention (only for reactive setting), (2) removing RAG by replacing Retrieved Causal Attention with self-attention, (3) removing the triplet loss $\mathcal{L}_{triplet}$, and (4) substituting high-level Jukebox features with Mel-spectrograms. Results show clear performance drops across most metrics, highlighting the importance of anticipatory modeling, retrieval grounding, and rich audio features for high-quality reactive motion generation. Please refer to Appendix for more ablation results.

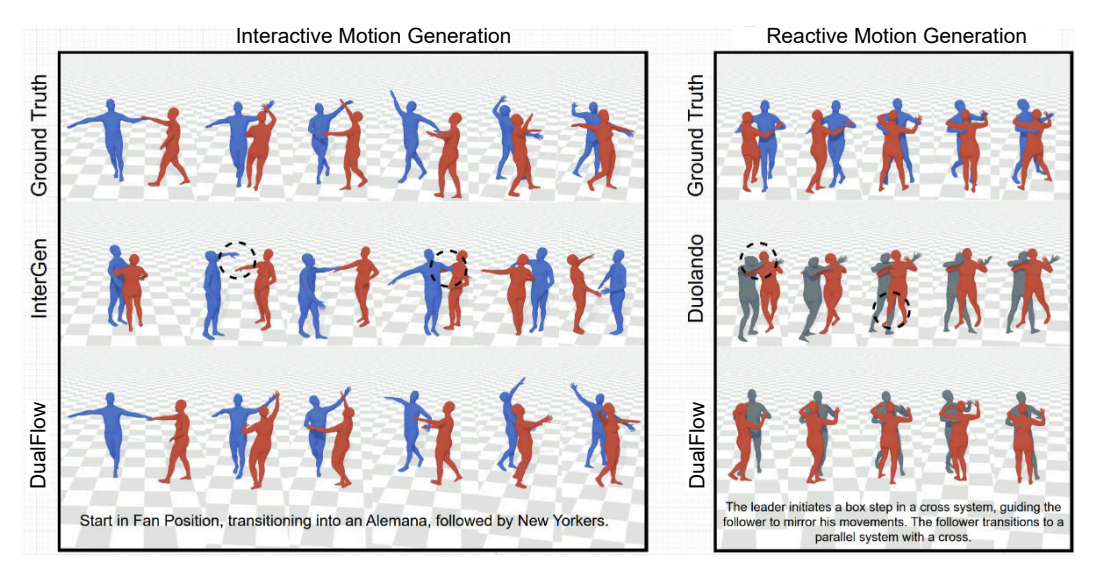


Figure 5: Comparing DualFlow with InterGen (interactive) and DuoLando (reactive) against ground truth on MDD Dataset. Black circles mark regions where baselines lose contact or produce distortions. InterGen shows artifacts like unnatural hand spacing, body interpenetration, and skipping the Alemana (follower's inside turn), while DuoLando shows incorrect leg initiation and head orientation. In contrast, DualFlow generates smooth, text-aligned choreography and coherent partner responses closely matching the ground truth. Supplementary video provides detailed visualizations.

Table 4: Ablation Study on MDD dataset (both text & music).

Methods	R	Precisio	n†	FID↓	MMDist↓	$\mathbf{Diverse} {\rightarrow}$	MModal↑	BED ↑	BAS↑
	Top 1	Top 2	Top 3						
Ground Truth	0.231	0.398	0.522	0.065	0.077	1.387	-	0.327	0.170
Interactive Task									
$\begin{array}{c} \text{DualFlow}(\text{w/o RAG}) \\ \text{DualFlow}(\text{w/o } \mathcal{L}_{\text{triplet}}) \\ \text{DualFlow}(\text{w/o } \mathcal{L}_{\text{sync}}) \\ \text{DualFlow}(\text{Spectral}) \\ \text{DualFlow}(\text{Jukebox}) \end{array}$	0.179 0.158 <u>0.182</u> 0.172 0.185	0.356 0.297 <u>0.369</u> 0.321 0.373	0.498 0.412 0.515 477 <u>0.513</u>	0.622 0.783 0.412 0.647 <u>0.415</u>	0.626 0.818 0.482 0.633 <u>0.513</u>	1.502 1.433 1.224 1.383 1.392	1.224 0.844 <u>1.340</u> 1.114 1.467	0.254 0.291 0.277 0.255 <u>0.286</u>	0.162 0.169 0.182 0.158 <u>0.179</u>
Reactive Task									
$\begin{array}{c} \text{DualFlow(w/o CLA)} \\ \text{DualFlow(w/o RAG)} \\ \text{DualFlow(w/o } \mathcal{L}_{\text{triplet}}) \\ \text{DualFlow(w/o } \mathcal{L}_{\text{sync}}) \\ \text{DualFlow(Spectral)} \\ \text{DualFlow(Jukebox)} \end{array}$	0.172 0.192 0.153 0.166 0.162 <u>0.189</u>	0.311 0.352 0.292 0.311 0.301 <u>0.341</u>	0.338 0.479 0.308 0.453 0.468 <u>0.471</u>	0.849 0.714 0.885 0.774 0.721 0.686	0.831 0.933 1.328 0.882 0.665 1.056	1.137 1.270 1.664 1.429 1.261 1.203	1.385 <u>1.466</u> 1.007 1.233 1.401 1.473	0.247 0.233 0.204 0.235 0.255 0.215	0.142 0.193 0.186 <u>0.202</u> 0.162 0.226

5 Conclusion

We introduced DualFlow, a unified rectified flow-based framework for efficient and expressive twoperson 3D motion generation, supporting both interactive and reactive settings with text, music, and retrieved motion exemplars. Leveraging rectified flow enables faster sampling and lower latency than diffusion-based methods. Extensive evaluations on MDD, InterHuman-AS, and DD100 show superior performance in duet generation and reactive motion. DualFlow advances multi-modal twoperson motion synthesis, opening new opportunities for immersive avatar interaction, intelligent choreography, and responsive digital humans. Future work will explore improved interactive generation with newer flow-matching methods, real-time motion editing, and few-shot adaptation to novel styles and languages.

REFERENCES

- Léore Bensabath, Mathis Petrovich, and Gul Varol. A cross-dataset study for text-based 3d human motion retrieval. In *Proceedings of the IEEE/CVF Conference on Computer Vision and Pattern Recognition*, pp. 1932–1940, 2024.
- Andreas Blattmann, Robin Rombach, Kaan Oktay, Jonas Müller, and Björn Ommer. Retrieval-augmented diffusion models. *Advances in Neural Information Processing Systems*, 35:15309–15324, 2022.
- Manolo Canales Cuba and João Paulo Gois. Flowmotion: Target-predictive flow matching for realistic text-driven human motion generation. *arXiv e-prints*, pp. arXiv–2504, 2025.
- Yuxuan Cao, Jiawei Ren, et al. Diffmotion: Conditional motion generation with diffusion models. In *CVPR*, 2023.
- Zhi Cen, Huaijin Pi, Sida Peng, Qing Shuai, Yujun Shen, Hujun Bao, Xiaowei Zhou, and Ruizhen Hu. Ready-to-react: Online reaction policy for two-character interaction generation. *arXiv* preprint arXiv:2502.20370, 2025.
- Wenhu Chen, Hexiang Hu, Chitwan Saharia, and William W Cohen. Re-imagen: Retrieval-augmented text-to-image generator. *arXiv preprint arXiv:2209.14491*, 2022.
- Rishabh Dabral, Muhammad Hamza Mughal, Vladislav Golyanik, and Christian Theobalt. Mofusion: A framework for denoising-diffusion-based motion synthesis. In *Computer Vision and Pattern Recognition (CVPR)*, 2023.
- Prafulla Dhariwal, Heewoo Jun, Christine Payne, Jong Wook Kim, Alec Radford, and Ilya Sutskever. Jukebox: A generative model for music. *arXiv preprint arXiv:2005.00341*, 2020.
- Yilun Duan, Joshua B Tenenbaum, et al. Multi-modal motion generation for embodied ai via transformers. *arXiv preprint arXiv:2204.08718*, 2022.
- Yunfan Gao, Yun Xiong, Xinyu Gao, Kangxiang Jia, Jinliu Pan, Yuxi Bi, Yixin Dai, Jiawei Sun, Haofen Wang, and Haofen Wang. Retrieval-augmented generation for large language models: A survey. *arXiv preprint arXiv:2312.10997*, 2(1), 2023.
- Anindita Ghosh, Rishabh Dabral, Vladislav Golyanik, Christian Theobalt, and Philipp Slusallek. Remos: 3d motion-conditioned reaction synthesis for two-person interactions. In *European Conference on Computer Vision*, pp. 418–437. Springer, 2024.
- Anindita Ghosh, Bing Zhou, Rishabh Dabral, Jian Wang, Vladislav Golyanik, Christian Theobalt, Philipp Slusallek, and Chuan Guo. Duetgen: Music driven two-person dance generation via hierarchical masked modeling. In *Proceedings of the Special Interest Group on Computer Graphics and Interactive Techniques Conference Conference Papers*, pp. 1–11, 2025.
- Chuan Guo, Shihao Zou, Xinxin Zuo, Sen Wang, Wei Ji, Xingyu Li, and Li Cheng. Generating diverse and natural 3d human motions from text. In *Proceedings of the IEEE/CVF conference on computer vision and pattern recognition*, pp. 5152–5161, 2022.
- Prerit Gupta, Jason Alexander Fotso-Puepi, Zhengyuan Li, Jay Mehta, and Aniket Bera. Mdd: A dataset for text-and-music conditioned duet dance generation. *arXiv preprint arXiv:2508.16911*, 2025.
- Kelvin Guu, Kenton Lee, Zora Tung, Panupong Pasupat, and Mingwei Chang. Retrieval augmented
 language model pre-training. In *International conference on machine learning*, pp. 3929–3938.
 PMLR, 2020.
- Yingqing He, Menghan Xia, Haoxin Chen, Xiaodong Cun, Yuan Gong, Jinbo Xing, Yong Zhang, Xintao Wang, Chao Weng, Ying Shan, et al. Animate-a-story: Storytelling with retrieval-augmented video generation. *arXiv preprint arXiv:2307.06940*, 2023.
 - Dan Hendrycks and Kevin Gimpel. Gaussian error linear units (gelus), 2023. URL https://arxiv.org/abs/1606.08415.

- Daniel Holden, Jun Saito, and Taku Komura. A deep learning framework for character motion synthesis and editing. *ACM Transactions on Graphics (TOG)*, 35(4):1–11, 2016.
- Vincent Tao Hu, Wenzhe Yin, Pingchuan Ma, Yunlu Chen, Basura Fernando, Yuki M Asano, Efstratios Gavves, Pascal Mettes, Bjorn Ommer, and Cees GM Snoek. Motion flow matching for human motion synthesis and editing. *arXiv* preprint arXiv:2312.08895, 2023.
 - Aaron Hurst, Adam Lerer, Adam P Goucher, Adam Perelman, Aditya Ramesh, Aidan Clark, AJ Ostrow, Akila Welihinda, Alan Hayes, Alec Radford, et al. Gpt-4o system card. arXiv preprint arXiv:2410.21276, 2024.
 - Sai Shashank Kalakonda, Shubh Maheshwari, and Ravi Kiran Sarvadevabhatla. Morag multifusion retrieval augmented generation for human motion. In *Proceedings of the IEEE/CVF Winter Conference on Applications of Computer Vision (WACV)*, 2025.
 - Jogendra Nath Kundu, Himanshu Buckchash, Priyanka Mandikal, Rahul M V, Anirudh Jamkhandi, and R. Venkatesh Babu. Cross-conditioned recurrent networks for long-term synthesis of interperson human motion interactions. In 2020 IEEE Winter Conference on Applications of Computer Vision (WACV), pp. 2713–2722, 2020. doi: 10.1109/WACV45572.2020.9093627.
 - Rudolf von Laban. *The mastery of movement on the stage*. Macdonald & Evans, 1950. URL https://cir.nii.ac.jp/crid/1130282272753007360.
 - Patrick Lewis, Ethan Perez, Aleksandra Piktus, Fabio Petroni, Vladimir Karpukhin, Naman Goyal, Heinrich Küttler, Mike Lewis, Wen-tau Yih, Tim Rocktäschel, et al. Retrieval-augmented generation for knowledge-intensive nlp tasks. *Advances in neural information processing systems*, 33: 9459–9474, 2020.
 - Boyuan Li, Xihua Wang, Ruihua Song, and Wenbing Huang. Two-in-one: Unified multi-person interactive motion generation by latent diffusion transformer, 2024a. URL https://arxiv.org/abs/2412.16670.
 - Ronghui Li, Youliang Zhang, Yachao Zhang, Yuxiang Zhang, Mingyang Su, Jie Guo, Ziwei Liu, Yebin Liu, and Xiu Li. Interdance: Reactive 3d dance generation with realistic duet interactions. *arXiv preprint arXiv:2412.16982*, 2024b.
 - Han Liang, Wenqian Zhang, Wenxuan Li, Jingyi Yu, and Lan Xu. Intergen: Diffusion-based multihuman motion generation under complex interactions. *International Journal of Computer Vision*, 132(9):3463–3483, 2024.
 - Zhouyingcheng Liao, Mingyuan Zhang, Wenjia Wang, Lei Yang, and Taku Komura. Rmd: A simple baseline for more general human motion generation via training-free retrieval-augmented motion diffuse. *arXiv preprint arXiv:2412.04343*, 2024.
 - Yaron Lipman, Ricky T. Q. Chen, Heli Ben-Hamu, Maximilian Nickel, and Matt Le. Flow matching for generative modeling, 2023. URL https://arxiv.org/abs/2210.02747.
 - Xingchao Liu, Chengyue Gong, and Qiang Liu. Flow straight and fast: Learning to generate and transfer data with rectified flow. *arXiv preprint arXiv:2209.03003*, 2022.
 - Matthew Loper, Naureen Mahmood, Javier Romero, Gerard Pons-Moll, and Michael J. Black. SMPL: A skinned multi-person linear model. *ACM Trans. Graphics (Proc. SIGGRAPH Asia)*, 34(6):248:1–248:16, October 2015.
 - Yinghao Lu, Tao Chen, et al. Real-time reactive motion synthesis with pre-trained motion models. *ACM TOG*, 41(6):1–12, 2022.
- Qianhui Men, Hubert PH Shum, Edmond SL Ho, and Howard Leung. Gan-based reactive motion synthesis with class-aware discriminators for human–human interaction. *Computers & Graphics*, 102:634–645, 2022.
 - Georgios Pavlakos, Vasileios Choutas, Nima Ghorbani, Timo Bolkart, Ahmed A. A. Osman, Dimitrios Tzionas, and Michael J. Black. Expressive body capture: 3D hands, face, and body from a single image. In *Proceedings IEEE Conf. on Computer Vision and Pattern Recognition (CVPR)*, pp. 10975–10985, 2019.

- Mathis Petrovich, Michael J Black, and Gül Varol. Temos: Generating diverse human motions from textual descriptions. In *European Conference on Computer Vision*, pp. 480–497. Springer, 2022.
 - Mathis Petrovich, Michael J. Black, and Gül Varol. Tmr: Text-to-motion retrieval using contrastive 3d human motion synthesis. In *Proceedings of the IEEE/CVF International Conference on Computer Vision (ICCV)*, pp. 9488–9497, October 2023.
 - Alec Radford, Jong Wook Kim, Chris Hallacy, Aditya Ramesh, Gabriel Goh, Sandhini Agarwal, Girish Sastry, Amanda Askell, Pamela Mishkin, Jack Clark, Gretchen Krueger, and Ilya Sutskever. Learning transferable visual models from natural language supervision. In Marina Meila and Tong Zhang (eds.), *Proceedings of the 38th International Conference on Machine Learning*, volume 139 of *Proceedings of Machine Learning Research*, pp. 8748–8763. PMLR, 18–24 Jul 2021.
 - Md Ashiqur Rahman, Jasorsi Ghosh, Hrishikesh Viswanath, Kamyar Azizzadenesheli, and Aniket Bera. Pacmo: Partner dependent human motion generation in dyadic human activity using neural operators, 2022. URL https://arxiv.org/abs/2211.16210.
 - Yoni Shafir, Guy Tevet, Roy Kapon, and Amit Haim Bermano. Human motion diffusion as a generative prior. In *The Twelfth International Conference on Learning Representations*, 2024.
 - Shelly Sheynin, Oron Ashual, Adam Polyak, Uriel Singer, Oran Gafni, Eliya Nachmani, and Yaniv Taigman. Knn-diffusion: Image generation via large-scale retrieval. *arXiv preprint arXiv:2204.02849*, 2022.
 - Li Siyao, Tianpei Gu, Zhitao Yang, Zhengyu Lin, Ziwei Liu, Henghui Ding, Lei Yang, and Chen Change Loy. Duolando: Follower gpt with off-policy reinforcement learning for dance accompaniment. *arXiv preprint arXiv:2403.18811*, 2024.
 - George Stoica, Vivek Ramanujan, Xiang Fan, Ali Farhadi, Ranjay Krishna, and Judy Hoffman. Contrastive flow matching. *arXiv* preprint arXiv:2506.05350, 2025.
 - Guy Tevet, Sigal Raab, Brian Gordon, Yonatan Shafir, Daniel Cohen-Or, and Amit H Bermano. Human motion diffusion model. *arXiv preprint arXiv:2209.14916*, 2022.
 - Runqi Wang, Caoyuan Ma, Jian Zhao, Hanrui Xu, Dongfang Sun, Haoyang Chen, Lin Xiong, Zheng Wang, and Xuelong Li. Leader and follower: Interactive motion generation under trajectory constraints, 2025. URL https://arxiv.org/abs/2502.11563.
 - Kevin Xie, Tingwu Wang, Umar Iqbal, Yunrong Guo, Sanja Fidler, and Florian Shkurti. Physics-based human motion estimation and synthesis from videos. In *Proceedings of the IEEE/CVF International Conference on Computer Vision*, pp. 11532–11541, 2021.
 - Liang Xu, Ziyang Song, Dongliang Wang, Jing Su, Zhicheng Fang, Chenjing Ding, Weihao Gan, Yichao Yan, Xin Jin, Xiaokang Yang, et al. Actformer: A gan-based transformer towards general action-conditioned 3d human motion generation. ICCV, 2023.
 - Liang Xu, Yizhou Zhou, Yichao Yan, Xin Jin, Wenhan Zhu, Fengyun Rao, Xiaokang Yang, and Wenjun Zeng. Regennet: Towards human action-reaction synthesis. In *Proceedings of the IEEE/CVF Conference on Computer Vision and Pattern Recognition*, pp. 1759–1769, 2024.
 - Hongwei Yi, Justus Thies, Michael J Black, Xue Bin Peng, and Davis Rempe. Generating human interaction motions in scenes with text control. In *European Conference on Computer Vision*, pp. 246–263. Springer, 2024.
 - Mingyuan Zhang, Xinying Guo, Liang Pan, Zhongang Cai, Fangzhou Hong, Huirong Li, Lei Yang, and Ziwei Liu. Remodiffuse: Retrieval-augmented motion diffusion model. In *Proceedings of the IEEE/CVF International Conference on Computer Vision (ICCV)*, pp. 364–373, October 2023a.
- Mingyuan Zhang, Zhongang Cai, Liang Pan, Fangzhou Hong, Xinying Guo, Lei Yang, and Ziwei Liu. Motiondiffuse: Text-driven human motion generation with diffusion model. *IEEE transactions on pattern analysis and machine intelligence*, 46(6):4115–4128, 2024.
 - Yujun Zhang, Liang Zhang, et al. Motiondiffuse: Text-driven human motion generation with diffusion model. *ACM Transactions on Graphics (TOG)*, 42(4):1–14, 2023b.

A LLM DISCLOSURE

 LLMs were only used to polish the text and proof read the paper for grammatical errors. They were not used to generate any metrics or citations.

B REPRODUCIBILITY

Full code for this project along with the trained checkpoints for all tasks will be made open source and publicly available upon paper acceptance.

C LLM-BASED DECOMPOSITION

C.1 PROMPT DESIGN

We design a structured prompting framework for the LLM, which is detailed as follows:

- 1. **System prompt:** We instruct the model with the following directive:
 - "As a professional dance movement analyst, please break down the given textual description of a duet dancing movement for {genre} into three focused descriptions: (1) Spatial Relationships: physical positioning, orientation, handhold (2) Body Movement: key gestures, actions, specific body part movements (3) Rhythm: tempo, timing, rhythmic dancing style and stepping. Please refer to the provided documents for guidance."
- 2. Few-shot Examples: We provide a curated set of genre-specific examples (3 per genre) illustrating how input descriptions are manually decomposed into the three components. These examples were crafted by analyzing a diverse subset of textual annotations in the MDD dataset and annotating their corresponding focused descriptions through expert review.
- Reference Guidelines: To promote interpretive consistency, we supply a supporting document containing structured definitions and keyword clusters describing typical language and semantic categories associated with each duet motion aspect.

C.2 GENERATED FOCUSED DESCRIPTIONS

To enhance semantic grounding during retrieval, we leverage a Large Language Model (LLM) to decompose free-form textual prompts into structured, movement-relevant subcomponents. Drawing inspiration from Laban Movement Analysis (LMA), we extract three focused descriptions: *Spatial Relationship*, *Body Movement*, and *Rhythm*. This decomposition allows the system to perform more targeted motion retrieval by aligning each aspect of the prompt with corresponding motion features. By translating ambiguous or abstract user descriptions into focused representations, the objective for the LLM-based refinement is to improve both retrieval precision and downstream motion generation quality. Table 5 shows some of the examples for the focused textual descriptions for text prompts for the MDD Dataset.

D MODEL ARCHITECTURE DETAILS

The proposed framework for duet and reactive motion generation employs a rectified flow matching approach. Our model utilizes transformer-based architectures with multi-scale temporal modeling and attention mechanisms, supporting optional text and music conditioning. The following section discusses about specific modules used in detail.

D.1 DUALFLOW BLOCK.

The DualFlow block applies multi-scale temporal convolutions with learnable gating:

$$\mathbf{f}_b^{(k)} = \text{GELU}(\text{Conv1D}_k(\mathbf{z}_b^{(j)\top}))^\top, \quad k \in \{1, 2, 3\}, \quad \mathbf{z}_b^{(j')} = \mathbf{z}_b^{(j)} + \sum_{k=1}^{3} \gamma_k \mathbf{f}_b^{(k)},$$

Table 5: Examples of input text decomposed into three fine-grained, semantically focused descriptions using LLM for MDD Dataset.

Total Description	C41 D-14	Dada Massas	Dhadhaa
Text Description	Spatial Relationship	Body Movement	Rhythm
The leader switches the hand hold from left to right, lead- ing the follower into a triple spin, maintaining a strong frame and connection.	The dancers are in an Open position with a Hand-to-hand connection. The leader switches the hand hold from left to right, maintaining a strong frame. They are facing each other during the transition.	The leader uses a strong frame to guide the follower into a triple spin. The follower's arms and torso are actively involved in the spinning motion, with medium energy.	The movement is executed at a fast tempo, with the triple spin occurring in quick succession, maintaining a continuous flow.
The dancers perform Jive Spanish Arms, maintaining a strong frame and connec- tion, with the follower exe- cuting a controlled turn.	The dancers are in a Closed position, facing each other with a strong Hand-to-hand connection. The leader maintains a firm frame, guiding the follower through the movement.	The leader maintains a steady posture, using arms and shoulders to guide. The follower performs a controlled turn, involving a smooth rotation of the torso and arms, with medium energy.	The movement is executed at a fast tempo, characteristic of Jive, with a continuous and lively rhythm, ensuring the turn is seamlessly integrated into the dance sequence.
From a separated position, the leader draws the fol- lower into a Closed Hand Hold, and they rotate clock- wise together.	The dancers transition from a separated position to a Closed position with a Hand-to-hand connection. They are facing each other as they move into this position.	The leader initiates a drawing motion, pulling the follower towards him. Both dancers engage in a rotating movement, turning their bodies clockwise together.	The rotation is performed at a medium tempo, with a continuous and fluid motion as they move in sync with each other.
The leader brings the fol- lower back with a circular motion, leading a head roll with his left hand, connect- ing it with a forward body roll for the follower. They then perform a basic step.	The dancers are in an Open position, with the leader facing the follower. They maintain a Hand-to-head connection as the leader guides the follower's head roll.	The leader uses his left hand to guide a head roll, involving the follower's head and neck. The follower transitions into a forward body roll, engaging the shoulders and torso. Both then perform a basic step, involving coordinated leg and foot movements.	The sequence begins with a medium-paced circular motion, transitioning into a fluid head and body roll. The basic step follows a steady, continuous tempo, maintaining rhythmic consistency.
The lead pulls the follow towards him, taking three steps, while the follow also takes three steps towards the lead. Both hands of both dancers are now connected.	The dancers are in a Closed position, facing each other. They have a Hand-to-hand connection with both hands engaged.	The lead and follow are both taking three steps towards each other. The movement involves the legs and feet, with a medium energy as they close the distance.	The steps are taken at a medium tempo, with each step evenly spaced, creating a continuous and synchronized rhythm between the dancers.

756

Each block applies a sequence of self- and cross-attention layers with residual connections and LayerNorm conditioning using the text latent \mathbf{z}_d . Let $\mathrm{LN}(\cdot,\mathbf{z}_d)$ denote LayerNorm with textconditioned shift/scale, and $\operatorname{Attn}(\mathbf{Q}, \mathbf{K}, \mathbf{V}) = \operatorname{softmax}(\frac{\mathbf{Q}\mathbf{K}^{\mathsf{T}}}{\sqrt{d}})\mathbf{V}$. The transformations applied are Self-Attention (equation 6), Music Cross Attention (equation 7), Motion Cross Attention (equation 8), Retrieval Cross Attention (equation 9), and Feedforward (FFN) Layer (equation 10):

 $\mathbf{z}_{a}^{(j,1)} = \mathbf{z}_{a}^{(j')} + \operatorname{Attn}(\mathbf{Q} = \operatorname{LN}(\mathbf{z}_{a}^{(j')}, \mathbf{z}_{d}), \mathbf{K} = \operatorname{LN}(\mathbf{z}_{a}^{(j')}, \mathbf{z}_{d}), \mathbf{V} = \operatorname{LN}(\mathbf{z}_{a}^{(j')}, \mathbf{z}_{d}))$

761

762

763

772

775

777

783

797

764

767 768 769

771

774

776

778

780 781

782

786

788

789 790 791

792 793 794

799 800 801

765 766

770

773

779

784 785

787

D.3

795 796

798

802

803 804 805

806 807

808

 $\mathbf{z}_{a}^{(j,2)} = \mathbf{z}_{a}^{(j,1)} + \operatorname{Attn}(\mathbf{Q} = \operatorname{LN}(\mathbf{z}_{a}^{(j,1)}, \mathbf{z}_{d}), \mathbf{K} = \mathbf{z}_{m}, \mathbf{V} = \mathbf{z}_{m})$

 $\mathbf{z}_{a}^{(j,3)} = \mathbf{z}_{a}^{(j,2)} + \operatorname{Attn}(\mathbf{Q} = \operatorname{LN}(\mathbf{z}_{a}^{(j,2)}, \mathbf{z}_{d}), \mathbf{K} = \mathbf{z}_{b}^{(j,2)}, \mathbf{V} = \mathbf{z}_{b}^{(j,2)})$

 $\mathbf{z}_a^{(j,4)} = \mathbf{z}_a^{(j,3)} + \operatorname{Attn}(\mathbf{Q} = \operatorname{LN}(\mathbf{z}_a^{(j,3)}, \mathbf{z}_d), \mathbf{K} = \mathbf{z}_R, \ \mathbf{V} = \mathbf{z}_R)$

 $\mathbf{z}_{a}^{(j+1)} = \mathbf{z}_{a}^{(j,4)} + FFN(LN(\mathbf{z}_{a}^{(j,4)}, \mathbf{z}_{d})),$

(6)

(7)

(8)

(9)

(10)

with symmetric updates for $\mathbf{z}_{b}^{(j)}$.

D.2 Interactive Setting

The flow dynamics are defined as:

$$\mathbf{x}(t) = [\mathbf{x}_a(t); \mathbf{x}_b(t)], \quad \mathbf{v}_{\theta}(\mathbf{x}(t), t, c) = [\mathbf{v}_{\theta, a}(\mathbf{x}(t), t, c); \mathbf{v}_{\theta, b}(\mathbf{x}(t), t, c)].$$

The final motion latents $\mathbf{z}_a^{(N)}$ and $\mathbf{z}_b^{(N)}$ are mapped to velocity fields

$$\mathbf{v}_{\theta,a} = \operatorname{Linear}(\mathbf{z}_a^{(N)}), \quad \mathbf{v}_{\theta,b} = \operatorname{Linear}(\mathbf{z}_b^{(N)}),$$
 (11)

concatenated as

$$\mathbf{v}_{\theta} = [\mathbf{v}_{\theta,a}; \mathbf{v}_{\theta,b}] \in \mathbb{R}^{B \times T \times 524}.$$
 (12)

REACTIVE SETTING

For reactive motion generation, our model generates the reactor's motion x_b conditioned on the actor's fixed motion x_a , with the flow dynamics defined as:

$$\mathbf{x}(t) = [\mathbf{x}_a; \mathbf{x}_b(t)], \quad \mathbf{v}_{\theta}(\mathbf{x}(t), t, c) = [\mathbf{0}; \mathbf{v}_{\theta, \text{reactor}}(\mathbf{x}(t), t, c)].$$

The Motion Cross Attention gets replaced by Causal Cross Attention in the DualFlow block for this setting. The final reactor latent $\mathbf{z}_b^{(N)}$ is mapped to the velocity field $\mathbf{v}_{\theta, \text{reactor}} = \text{Linear}_L^{262}(\mathbf{z}_b^{(N)})$, and the output is $\mathbf{v}_{\theta} = [\mathbf{0}; \mathbf{v}_{\theta, \text{reactor}}] \in \mathbb{R}^{B \times T \times 524}$. During inference, the initial state is $\mathbf{x}(0) = [\mathbf{x}_a; \mathbf{z}_b]$, where $\mathbf{z}_b \sim \mathcal{N}(\mathbf{0}, \mathbf{I})$.

CAUSAL CROSS ATTENTION WITH LOOK-AHEAD

The Causal Cross Attention module enables the reactor to condition on the actor's motion while preserving temporal causality and allowing limited future anticipation. For reactor motion latent $\mathbf{z}_{b}^{(j,2)}$ and fixed actor motion latent \mathbf{z}_{a} from DualFlow block j, we construct query, key, and value matrices as $\mathbf{Q} = \mathbf{z}_b^{(j,2)} \mathbf{W}_Q$, $\mathbf{K} = \mathbf{z}_a \mathbf{W}_K$, and $\mathbf{V} = \mathbf{z}_a \mathbf{W}_V$, where \mathbf{W}_Q , \mathbf{W}_K , and $\mathbf{W}_V \in$ $\mathbb{R}^{L \times d_k}$ are learned projection matrices. The causal mask with look-ahead parameter L uses an upper triangular mask such that reactor's motion attends to past and only L future frames of the actor's motion, implemented as $\mathbf{M}_{i,j} = 1$ if $j \leq i + L$ and $\mathbf{M}_{i,j} = 0$ otherwise. The attention computation follows:

$$\text{CausalCrossAttention}(\mathbf{Q}, \mathbf{K}, \mathbf{V}) = \text{softmax}\left(\frac{\mathbf{Q}\mathbf{K}^T}{\sqrt{d_k}}\odot\mathbf{M} + (1-\mathbf{M})\cdot(-\infty)\right)\mathbf{V}$$

where \odot denotes element-wise multiplication. This formulation ensures temporally aligned and context-aware reactive generation, enabling natural reactive responses that align with the actor's intended trajectory without violating temporal consistency.

D.5 MODEL PARAMETERS

Loss Weighting Values We assign higher weights to geometric losses for velocity ($\lambda_{\text{vel}} = 30$) and foot contact ($\lambda_{\text{foot}} = 30$), moderate weight for bone length consistency ($\lambda_{\text{BL}} = 10$), and emphasize inter-dancer synchronization ($\lambda_{\text{sync}} = 5$). Affinity and distance are equally weighted ($\lambda_{\text{DM}} = 3$), while orientation receives a minimal weight ($\lambda_{\text{RO}} = 0.01$). These settings ensure anatomically plausible, temporally smooth, and well-coordinated duet motions.

E QUANTITATIVE EVALUATION

We further conduct ablations to study model design choices: (1) replacing the three temporally scaled parallel convolutions with a single convolution, (2) reducing the number of transformer blocks to 10 and 15 (from 20), and (3) lowering the latent dimension to 128 and 256 (from 1024). These variants consistently show performance drops across most metrics, highlighting the benefit of the full architecture.

Table 6: Ablation study results for ReactFlow

Methods	R-	R-Precision [†]		FID↓	MMDist↓	$\textbf{Diversity}{\rightarrow}$	MModal [†]	BED ↑	BAS↑
	Top 1	Top 2	Top 3						
Ground Truth	0.231	0.398	0.522	0.065	0.077	1.387	-	0.327	0.170
DualFlow (one conv)	0.172	0.311	0.338	0.595	0.582	1.288	1.385	0.266	0.142
DualFlow (10 blocks)	0.160	0.313	0.452	0.683	0.654	1.215	1.222	0.259	0.159
DualFlow (15 blocks)	0.175	0.357	0.521	0.482	0.627	1.211	1.402	0.270	0.163
DualFlow (128 latent)	0.108	0.284	0.414	0.966	0.834	1.277	1.091	0.273	0.141
DualFlow (256 latent)	0.168	0.342	0.468	0.642	0.681	1.245	1.328	0.291	0.163
DualFlow	0.185	0.373	0.513	0.415	0.513	1.307	1.467	0.286	0.179

Performance decrease in different settings shows the importance of 3 parallel temporal Convs, using 20 blocks, 515 Latent dimension and Jukebox embeddings for music. Here, **Bold** indicates the best result

F QUALITATIVE EVALUATION

User Study Details. A total of 24 participants were recruited for the study. Each participant is shown 15 pairs of rendered videos (3 per experiment), with each video lasting less than 10 seconds. Each pair consists of one motion sequence generated by DualFlow and the other by either a baseline method or the ground truth (when available). To ensure unbiased evaluation, the order of videos within each pair is randomized, and no method labels are revealed. For each video pair, participants are asked to answer three key questions: (1) Which motion better aligns semantically with the textual description? (2) Which motion is better synchronized with the musical beats? (3) Which motion has higher overall quality (e.g., naturalness, smoothness etc)? Fig.6 shows the User Study Form we used.

Fig. 6 illustrates the User Study Form presented to participants during the human evaluation study. Clear and detailed guidelines were provided at the beginning of the form, explaining the evaluation criteria. Participants were then asked to watch two videos: one containing motion from either a Baseline model or the Ground Truth, and the other generated using our DualFlow model. The identity of each video (i.e., whether it was from the DualFlow model or the comparison method) was not disclosed to the participants. For each experimental condition, participants viewed and evaluated three distinct pairs of videos.

User Study For DualFlow Motion	COMMERCIAL
Generation	
Dear Participant,	
Thank you for taking the time to participate in our user study!	
In this study, you will be shown two motion sequences for each comparison. Your task is o evaluate these sequences by answering three questions based on different aspects of motion quality. The sequences are from 3 different experiments namely Fext Alignment. TI, Musical Synchronization [Mi, Overall Motion Quality [O]. You will be shown 15 samples from each experiment. For each pair of motions, please select the one that you believe performs better on each of he following criteria: I. Text Alignment: Which motion better reflects the meaning of the textual description?	T1. Which motion more accurately reflects the meaning of the accompanying textual description? Sequence 1 Sequence 2
The motion closely reflects the actions, emotions, or scenario described. The meaning is clearly communicated through the body movements. The motion is contextually appropriate and logically consistent with the description.	M1. Which motion is better synchronized with the rhythm and beats of the
Musical Synchronization: Which motion is better synchronized with the rhythm and beats of the music?	background music?
Key movements occur in syne with musical beats and accents. The rhythm and pacing of the motion match the tempo of the music. The motion expresses changes in musical energy, such as shifts in mood or intensity.	Sequence 2
3. Overall Motion Quality: Which motion looks more natural and visually pleasing overall?	
Transitions between poses are smooth and continuous. Movements follow realistic and believable trajectories. The motion is visually coherent, expressive, and aesthetically pleasing.	O1. Which motion looks more natural and visually pleasing overall? Sequence 1
Please answer thoughtfully based on your perception. Your evaluations will be valuable to	Sequence 2

Figure 6: User Study Google Form